# Flexibility of F-Actin in Aqueous Solution: A Study on Filaments of Different Average Lengths

**J. Drögemeier, H. Hinssen,† and W. Eimer***

*Department of Chemistry, University of Bielefeld and Cell Biology Group, D-33615 Bielefeld, Germany*

*Received January 19, 1993; Revised Manuscript Received October 14, 1993*•

ABSTRACT: We have investigated the dynamics of F-actin with different average filament lengths in dilute and semidilute solution by polarized dynamic light scattering. The average degree of polymerization, $\langle X \rangle$, of F-actin was controlled by the actin-binding protein gelsolin. By variation of the molar ratio of actin/gelsolin, we obtained a homologous series of filaments with $50 < \langle X \rangle < 2000$, the polydispersity of the system being characterized by an exponential distribution. Comparison of the electric field autocorrelation function decay profile in the dilute regime with model calculations for rigid and semiflexible rodlike polymers revealed that the microfilaments are rather stiff molecules. From measurements on the homologous series of different filament lengths the persistence length was determined to $P = 7.5 \pm 2.5$ μm. The contribution of internal bending motions to the correlation funtion was clearly discernible for longer filaments and at larger scattering vector, respectively. To characterize the concentration effect on the polarized dynamic structure factor, we studied solutions with $\langle X \rangle = 350$ from 2.2 to 105 μM actin. The transition from dilute to semidilute regime was detected at $c\langle L \rangle^3 \approx 15$. This is very similar to findings on other polymer systems with a narrower size distribution. While at low scattering angle the apparent diffusion coefficient is independent on concentration, we observed a decrease of $D_{app}$ at $\theta = 90°$. From this we concluded that the rotational motion of the rodlike molecules is restricted at higher $c\langle L \rangle^3$. In addition, with increasing concentration a slow mode appeared in the experimental correlation functions. The amplitude decreased with increasing scattering vector. The nature of the slow relaxation process, also observed in other polymer systems, is still under debate.

## Introduction

The 42-kDa protein actin is one of the major components in muscle and nonmuscle cells. In polymerized form, filamentous or F-actin, governs the structural organization and viscoelastic properties of the cytoskeleton.[1,2] As a consequence, the microfilaments play an important role in cellular transport processes. Because the filament network is anchored to the plasma membrane, it also controls the shape of the cell, and hence cell locomotion and division.[3] These manifold functions can be fulfilled only in cooperation with a large number of actin-binding proteins that regulate the filament length and consistency of the network.[4]

For a better understanding of the biological function, the dynamic and viscoelastic properties of the actin filaments are of profound interest. Different experimental approaches like rheology and mobility studies lead to controversial conclusions concerning the viscoelastic behavior in solution. On one hand, the experimental results were discussed in terms of an infinite network of highly flexible polymer molecules.[5,6] In an alternative approach the microfilaments were considered to be rodlike without cross-links and the dynamic behavior was attributed to hindered diffusion of the stiff molecules due to steric hindrance.[7,8] For very long molecules however, it becomes rather difficult to distinguish between networks of stiff macromolecules and an entangled system of cross-linked flexible polymers, respectively. At high concentration, the rotational motion of rigid filaments is severely restricted, and orientation of the molecules will result in liquid–crystal-like structures. If however the lengthwise motion of the long molecules becomes also highly restricted, orientation of the isotropic phase will be prevented.[9]

Previous dynamic light scattering studies[10–14] have been performed mostly on filamentous actin or complexes with actin-binding proteins to obtain information about the flexibility of the microfilaments. Because the polymerization of actin leads to very long helical structures, it is obvious that the system exhibits a quite complex dynamic behavior, including diffusional motions of shorter filaments or chain segments as well as local internal motions of the polymer. In addition, concentration effects on these relaxation modes, caused by steric repulsion and inter- and intramolecular interactions, together with the polydispersity of the system, complicate the analysis of the experimental data.

To circumvent some of these problems involved in studying pure F-actin, we have polymerized G-actin in the presence of gelsolin, an actin-binding protein that is known to cap and sever actin filaments.[15–17] Variation of the molar ratio of actin to gelsolin provided filaments with an average length that is over a wide range proportional to the gelsolin concentration.[18]

In extension to a previous DLS study by Janmey et al.,[19] we have performed detailed angular dependent measurements on actin/gelsolin solutions with an average degree of polymerization between 50 and almost 2000 monomer units. In the dilute solution regime we compared the entire decay profile of the experimental correlation functions with model calculations for rigid[20] and semiflexible rodlike[21,22] macromolecules. Concentration-dependent measurements gave valuable information about the dynamic behavior of the actin filaments in semidilute solution.

Besides the biological interest, we have chosen the microfilaments as an interesting model system to test the theoretical expressions for the polarized dynamic structure factor of rigid and semiflexible rodlike polymers in solution.

* To whom correspondence should be addressed.
† Cell Biology Group.
• Abstract published in *Advance ACS Abstracts*, December 1, 1993.

0024-9297/94/2227-0087$04.50/0 

Data from light[23] and electron microscopy[24] suggest that actin filaments are one of the stiffest macromolecules, their persistence length being estimated to 3–15 μm. In the following paper[25] we will present a detailed depolarized dynamic light-scattering study on F-actin in solution to round out our comparison of experimental data with theoretical predictions on the correlation function profile.

## Theoretical Background

The theories on the dynamics of thin, rigid rodlike macromolecules have developed from the pioneering work of Pecora,[26] who considered rotational and translational motion in his model (for review see ref 27). In addition, the translational displacement of the stiff molecules depends on the orientation. This translational rotational coupling has been accounted for by many authors.[28–30] With increasing concentration of rod–rod interactions, topologic constraints and hydrodynamic interactions should affect the dynamics of the polymers. Within certain limits, Doi et al.[31] included all these effects to derive a theory for the dynamic structure factor of rigid rodlike molecules. Maeda[20] has rewritten these expressions in matrix form to calculate the dynamic structure factor in the entire region of the time, concentration, and scattering vector.

In the following we will briefly discuss the expressions obtained for the initial decay rate, $\Gamma_{init} \equiv -\lim_{t\to 0}[(d/dt)\, g(q,t)/g(q,0)]$, to illustrate the contribution of the different relaxation modes to the DLS spectra. The apparent diffusion coefficient, $D_{app} = \Gamma_{init}/q^2$, is given by

$$D = [D_0 + (L^2/12)\Theta_\perp f_1(qL) - (D_\parallel - D_\perp)[{}^1/_3 - f_2(qL)]]A(qL,c) \quad (1)$$

The first term in eq 1 considers the translational motion of the macromolecule where $D_0$ is the overall translational diffusion coefficient $D_0 = (D_\parallel + 2D_\perp)/3$. $D_\parallel$ and $D_\perp$ characterize the translational motion parallel and perpendicular to the rod axis, respectively. The second term results from rotational reorientation, where $\Theta$ is the rotational diffusion coefficient and $L$ the length of the rod. The last expression in parentheses describes the contribution from coupling of translational and rotation motion and leads to a decrease of the apparent diffusion coefficient. The weight factors $f_1$ and $f_2$ are known functions of $qL$.[32] The limiting values for $q \to 0$ and $q \to \infty$ are $f_1(0) = 0$, $f_1(\infty) = 1$ and $f_2(0) = {}^1/_3$, $f_2(\infty) = 0$, respectively. Therefore, at low $q$ value (low scattering angle) and for not too long molecules, $\Gamma_{init}/q^2$ gives the translational diffusion coefficient. $A(qL,c)$ expresses the excluded-volume effect, assuming hard core interactions between the rods, and is an increasing function of the number concentration, $c$. The interaction parameter is also $q$ dependent, with the most significant contribution in the forward scattering direction. The diffusion coefficients in eq 1 are considered as adjustable quantities to account for topological and hydrodynamic effects on the relaxation modes.

Most rodlike macromolecules exhibit some dynamic flexibility. These internal bending motions become evident at high scattering angle in the DLS experiment, in such a way, that the apparent diffusion coefficient increases beyond the expected value for a stiff molecule. Maeda and Fujime[21,22] have developed a theory that gives a quantitative description for free Brownian motion of semiflexible rods in dilute solution. The expression for the apparent diffusion coefficient, as obtained from the initial decay rate is given by

$$D_{app} = [D_0 + (L^2/12)\Theta_\perp f_1^*(qL) - (D_\parallel - D_\perp)[{}^1/_3 - f_2^*(qL)]] + \sum D_{[m]} a_m(q) \quad (2)$$

This equation is similar to eq 1 for rigid rodlike molecules, except for an additional term

$$\sum D_{[m]} a_m(q) \quad (3)$$

that describes the bending displacement of individual subunits in direction perpendicular to the rod axis. The $m$-th bending mode of the molecule is characterized by a diffusion coefficient

$$D_{[m]} = (kT/4\pi\eta_0 L)(1 + f_m^*(qL)) \quad (4)$$

where $m > 2$. The weight functions $f_m^*(qL)$ ($m = 1, 2, ..., m$) are also dependent on the flexibility of the molecules,[33,34] defined by the inverse Kuhn length

$$\gamma = kT/2\epsilon \quad (5)$$

where $\epsilon$ is a torque constant that describes the bending rigidity.

Expressions for the rotational and translational diffusion coefficients of rigid rodlike molecules have been developed by Tirado and Garcia de la Torre.[35–37] The correction factors for the transport coefficients of semiflexible macromolecules, $\Theta^{sfr} = \Theta^{rr} g(\gamma,L,d)$ and $D^{sfr}$ as well as an approximate relation for $(D_\perp^{sfr} - D_\parallel^{sfr})/D_0^{sfr}$ are known.[38–40]

The available theories for semiflexible rodlike macromolecules are still inadequate for a complete description of their dynamics. As Schurr and co-workers[41] already pointed out, using the Harris–Hearst model gives some internal inconsistencies. For example, first, the hydrodynamic interaction of the cylindrical elements was not taken properly into account by Fujime and Maeda, and second, the constant length of the molecules was not enforced. These effects introduce incorrect amplitudes and relaxation rates for the bending motions, and hence the rigid-rod result is not obtained in the limit of infinite bending rigidity. Aragon[42] has handled the constraint of constant length exactly which are correct in the rigid-rod limit. But he ignored hydrodynamic interactions, and what is more important, in case of the long actin filaments, his theory does not account for the coupling of rotational and translational motion. Therefore, we decided to compare our experimental results with the theory of Fujime and Maeda. The coupling of bending flexibility with rotational and translational motion of the semiflexible molecules has not yet been considered explicity. The reader should keep in mind that the state of theory for semirigid macromolecules is still deficient, and we want to encourage theoreticians to improve our understanding about the complex dynamics of these polymer molecules. The conclusions concerning the flexibility of the actin filaments from our work should be looked at from this point of view.

## Materials and Methods

**Sample Preparation.** Actin was isolated from rabbit skeletal muscle according to a modified method of Spudich and Watt.[43] For additional separation of G-actin from higher oligomers we added a gel chromatography over a G-150 Sephadex column. Gelsolin was prepared from smooth muscle pig stomach by a procedure described in detail by Hinssen et al.[44] and Pope et al.[45] For both proteins concentration was measured by the Biuret method.

G-Actin was stored in a low ionic strength buffer: 0.2 mM $CaCl_2$, 0.2 mM ATP, 0.2 mM β-mercaptoethanol, and 2 mM imidazole/HCl at pH 7.2. Prior to polymerization, gelsolin was added in the desired molar ration to induce nucleation, and the solution was filtered through 0.2-μm Anotec filters into a dust-

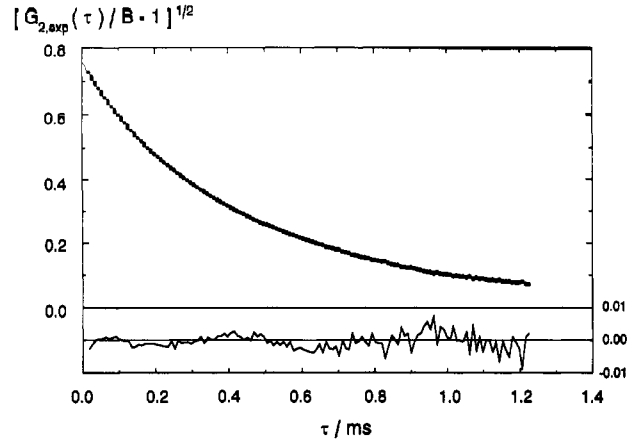


**Figure 1.** Typical experimental polarized electric field autocorrelation function analyzed with a fourth-order cumulant fit together with the residuals. [A]:[G] = 100; [A] = 5 $\mu$M; $\Theta$ = 90°.

free rectangular fluorescence cell. After addition of high ionic strength buffer (0.1 M KCl, 2 mM $MgCl_2$, 0.4 mM $CaCl_2$, 2 mM ATP, 0.2 mM $\beta$-mercaptoethanol, and 2 mM imidazole/HCl at pH 7.2) to initialize polymerization, the sample was centrifuged for 20 min at 1000$g$. The light scattering experiments were started about 90 min after polymerization. A set of experiments (angular dependence for a given actin:gelsolin ratio) lasted from 90 min to about 20 h, depending on the scattering intensity and number of scattering angles studied. During this period of time, the measured apparent diffusion coefficient was constant within 1–2%. In general, we observed a significant change in the diffusion coefficient at the earliest after $t > 24$ h, that is probably related to a biochemical instability of the proteins.

**Dynamic Light Scattering Measurements and Analysis.** We performed the dynamic light scattering measurements in the VV geometry: vertical polarization of the incident beam and detection of the vertically polarized scattered light. As a light source, we used an argon ion laser (Coherent; Model Innova 90-5) in single mode, operating at $\lambda$ = 488 nm. The scattered light was analyzed by a correlator from Brookhaven Inc.; model BI-2030. The correlator was run in the linear or multi-$\tau$ mode with a total of 142 data points including 6 delay channels (delayed by 1024 times the sample time). Data accumulation of the intensity autocorrelation function continued up to $\sim 10^7$ cts/channel. In general, only correlation functions with a baseline difference of less than 0.4% were accepted for further analysis. At low scattering angles, we measured time correlation functions for short periods of time ($2 \times 10^4$ to $1 \times 10^5$ cts/channel), and those with a difference in measured and calculated baseline higher than 0.5–1% (depending on scattering angle and intensity) were rejected. The accepted spectra were accumulated to a total of $10^7$ cts/channel. At high concentration, where we observed a slow mode, the accepted baseline difference increased to about 1%. DLS spectra were taken at different scattering angles 20° < $\theta$ < 120° and at a temperature of 10 °C.

For data analysis we used a fourth-order cumulant fit[46] to the experimental data. A typical DLS spectra together with the calculated fitting function is given in Figure 1. Inverse Laplace transformation of the normalized electric field autocorrelation function, as obtained according to $g^{(1)}(\tau) = [G^{(2)}(\tau)/B - 1]^{1/2}$, by CONTIN[47-49] provided in most cases a single peak with an amplitude of >75% and a broad distribution of relaxation rates. However, this method did not always give reproducible results, and therefore we used the cumulant analysis for comparison with the computed apparent diffusion coefficients from the model calculations. Our main conclusions are based on a direct comparison of the entire decay profile of calculated correlation functions with the experimental data.

**Simulation of VV Correlation Functions.** The calculations of the polarized dynamic light scattering spectra are based on the theory for rigid and semiflexible rodlike macromolecule by Fujime and Maeda (refs 21 and 22, respectively). For monodisperse samples, Maeda has written FORTRAN programs that compute the unnormalized polarized dynamic structure factor. We have altered his programs to account for the polydispersity of F-actin. In the following, we will briefly explain the modifications we made. The VV correlation function was calculated at 20 delay times with

$$\tau_1 = 0 \text{ s}$$
$$\tau_i = \sum_{i=2}^{i\le 20} (\Delta\tau) a^{i-2} \quad \text{for} \quad 2 \le i \le 20 \tag{6}$$

where $\Delta\tau$ is the sample time and $a$ = 1.55. The constant $a$ was introduced to cover a broader time range, necessary for appropriate consideration of the different filament lengths. $\Delta\tau$ was set to 50, 20, 5, 2, and 1.5 $\mu$s for the different scattering angles $\theta$ = 20°, 35°, 60°, 90°, and 120°. The delay times were chosen in accordance with the experimental sample times. Considering the polydispersity of the system, the VV correlation functions the unnormalized dynamic structure factor was obtained according to

$$g_{VV}(\tau_i) = \frac{\sum_{X=X_{min}}^{X_{max}} Y_X L_X{}^2 g_{VV}(L_X,\tau_i)}{\sum_{X=X_{min}}^{X_{max}} Y_X L_X{}^2} \tag{7}$$

by averaging over different degrees of polymerization, $X$, for the assumed distribution function, in our case an exponential length distribution. $Y_X$ is the mole fraction of filaments with length $L_X$.

Because the computational time for longer actin filaments increased rapidly, we used the following interpolation scheme for calculating the theoretical correlation functions. We first computed $G_{VV}(L_n,\tau_i) = g_{VV}(L_n,\tau_i)/G_D(L_X,\tau_i)$ for molecules with length

$$L_n = L_0 c^n \tag{8}$$

where $L_0$ = 11 nm is the length of the smallest actin/gelsolin complex considered (an actin dimer with an attached gelsolin molecule) and $c$ = 1.2. For the dimensions of the actin helix we assumed an increase in length by 2.77 nm[50] per monomer unit and a diameter of 10 nm.[51,52] $g_{VV}(L_n,\tau_i)$ is the unnormalized dynamic structure factor as defined in ref 21 for rigid and semiflexible macromolecule in dilute solution, and $G_D(L_n,\tau_i) = \exp[-q^2 D_n \tau]$ contains information about the translational motion of the macromolecule. We computed $G_{VV}(L_n,\tau_i) = g_{VV}(L_n,\tau_i)/G_D(L_n,\tau_i)$ of rigid rods and semiflexible molecules with a Kuhn length of 7.5, 10, 15, 20, and 30 $\mu$m for the above-mentioned scattering angles. $N$ varied between 39 and 45, depending on the flexibility and scattering angle. These calculations were performed on a Convex C240. The data were then stored on a HP 9000-300 workstation for a further evaluation of the individual correlation functions.

By cubic spline interpolation of $G_{VV}(L_n,\tau_i)$ versus ln $L_n$ we calculated the unnormalized dynamic structure factor $g_{VV}(L_X,\tau_i) = G_{VV}(L_n,\tau_i)G_D(L_n,\tau_i)$ for filaments with different degrees of polymerization $X$. For a given length distribution, $g_{VV}(\tau_i)$ was obtained according to eq 12 for the different scattering angles and flexibility parameters. And last, for comparison with the experimental data, we computed the normalized electric field autocorrelation function $g_1(\tau)$ by cubic spline interpolation of ln $[g_{VV}(\tau_i)/g_{VV}(0)]$ versus $\tau$. We chose 136 data points to obtain a decay profile similar to the experimental DLS spectra.

The translational and rotational diffusion coefficients for rigid rodlike macromolecule were calculated according to the theory of Tirado and García de la Torre.[35-37] For semiflexible rodlike macromolecule Yamakawa and Fujii derived a theory for the translational diffusion coefficient. The rotational diffusion coefficient for semiflexible rodlike macromolecule was evaluated by Hagerman and Zimm[40] from Monte Carlo simulations. More details on the model calculations are given in ref 53.

## Results and Discussion

To characterize the dynamics of actin filaments in solution we have measured intensity autocorrelation functions of the polarized component of scattered light

**Table 1. Characteristic Light Scattering Parameters for F-Actin Filaments of Different Average Filament Lengths**

| | [A]:[G] | | | | | |
|---|---|---|---|---|---|---|
| | 50 | 100 | 200 | 400 | 800 | 1600 |
| $c\langle L\rangle^{3}$ [a] | 0.052 | 0.21 | 0.83 | 3.3 | 13 | 53 |
| $c\langle L\rangle^{3}$ [b] | 0.13 | 0.53 | 2.1 | 8.5 | 34 | 136 |
| $\langle L\rangle$/nm | 140 | 280 | 560 | 1120 | 2240 | 4480 |
| $\gamma\langle L\rangle$ | 0.009 | 0.019 | 0.037 | 0.081 | 0.149 | 0.299 |
| $q\langle L\rangle$ [c] | 0.835 | 1.67 | 3.34 | 6.68 | 13.4 | 26.7 |
| $q\langle L\rangle$ [d] | 3.40 | 6.80 | 13.6 | 27.2 | 54.4 | 108.7 |

[a] Calculated for prep A with [A] = 2.5 μM. [b] Calculated for prep B with [A] = 5.0 μM. [c] Θ = 20°. [d] Θ = 90°.

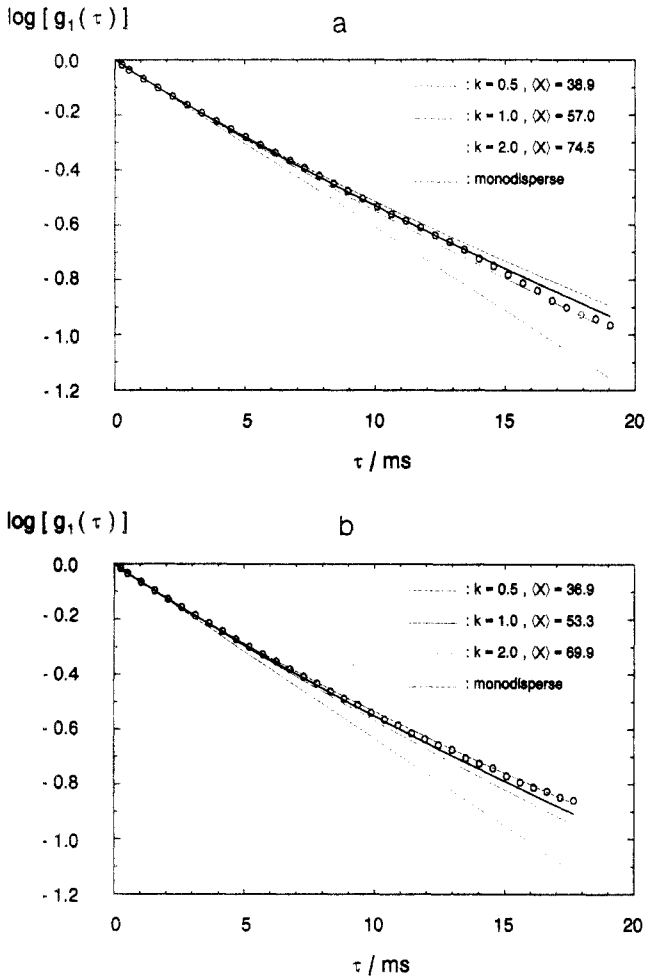


**Figure 2.** Comparison of an experimental first-order correlation function ([A]:[G] = 50, $\theta$ = 20°) with model calculations for rigid rods from two different preparations ([A] = 5 μM). We assumed a Schulz–Zimm distribution (see eq 9) with $k$ = 0.5, 1.0, 2.0, and ∞ (monodisperse sample).

for different average filament lengths by varying the molar ratio of actin/gelsolin from 50:1 to 1600:1. A general overview with the, in this context, most significant parameters for the dynamic light scattering study is given in Table 1. In extension to a previous study,[19] we performed angular dependent measurements and compared the experimental correlation functions with calculated data from polymer models for rigid and semiflexible macromolecule to obtain information on the flexibility of the actin filaments.

**Effect of Polydispersity.** The first problem we had to consider was the distribution of filament lengths for a given ratio of actin/gelsolin. The effect of polydispersity on the decay profile of the intensity autocorrelation function is demonstrated in Figure 2. The theoretical polarized DLS spectra was calculated assuming a Schulz–Zimm distribution,[54] where the number distribution is given by

$$Y_X = \frac{(k/\langle X\rangle)^{k+1} X^{k-1} \langle X\rangle \exp(-kX/\langle X\rangle)}{\Gamma(k+1)} \quad (9)$$

$\langle X\rangle$ is the average degree of polymerization, $\Gamma(k+1)$ the gamma function, and $k$ is characteristic for the width of the distribution function. For $k$ = 1 we obtain the exponential distribution and $k \to \infty$ corresponds to a monodisperse sample. Figure 2 gives a comparison of the experimental correlation function for a solution of actin/gelsolin 50:1 with calculated spectra for $k$ = 0.5, 1.0, 2.0, and ∞. The average degree of polymerization, $\langle X\rangle$, for the different distributions was chosen in such a way that the initial decay rate, $\Gamma_{init}$, for all, theoretical and experimental, correlation functions was identical within 0.2%. As Figure 2 reveals, the experimental correlation functions from both actin preparations are in good agreement with theoretical spectra for $k$ = 1. The assumption of an exponential distribution of filament length is supported by analysis of electron micrographs of actin/gelsolin assays.[19] Furthermore, Figure 2 illustrates that, for $0.5 \leq k \leq 2$, the broadness of the distribution has a minor effect on the decay profile considering the error in the experimental data for the longer times of the experimental correlation function. Therefore, in the following discussion we assumed an exponential distribution of filament lengths for calculating theoretical correlation functions.

**Flexibility of the F-Actin Filaments.** The angular dependence of the initial decay rate is a good indicator for any flexibility located in the actin filaments. According to eq 2, for a semiflexible macromolecule we would expect a stronger increase in $\Gamma_{init}$ with the scattering vector $q$ than for rigid rods. To elucidate the extent of flexibility of the filaments, we have performed DLS measurements on two different protein preparations, varying the actin/gelsolin ratio between 50:1 and 1600:1. The actin concentrations were 2.5 μM (prep A) and 5.0 μM (prep B), respectively. Figure 3 shows the dependence of the initial slope apparent diffusion coefficient, $D_{app} = \Gamma_{init}/q^2$, on the average degree of polymerization $\langle X\rangle$ at two different scattering angles ($\theta$ = 20° and $\theta$ = 90°). The initial decay rate was obtained from a fourth-order cumulant fit to the experimental data. For comparison, we have included calculated values for rigid rodlike macromolecule and semiflexible polymers with a statistical Kuhn length of $\gamma^{-1}$ = 7.5, 15, and 30 μm. The theoretical values for $D_{app}$ were also determined by a cumulant fit to the calculated correlation function instead of using eq 1 or 2, respectively. This was done to exclude any uncertainty related to the evaluation of the initial decay rate from the experimental correlations functions because of the limited number of data points at very short decay times. Figure 3a reveals that at low $q$ value and for short filaments the model calculations for rigid and semiflexible polymers are identical considering the experimental error in the DLS spectra. For longer filament lengths and higher scattering angles, respectively, (see Figure 3b) the experimentally determined apparent diffusion coefficients are significantly larger than expected for rigid rodlike macromolecule. The experimental data are in good agreement with model calculations assuming a persistence length, $P = 0.5\gamma^{-1}$, of 7.5 ± 2.5 μm.

For both actin concentrations and for the wide range of different average filament lengths studied, the experimental data are well represented by the same model parameters indicating that we obtained a consistent picture concerning the stiffness of F-actin of various lengths. Only for low scattering value, $\theta$ = 20°, and for the highest average degree of polymerization, $D_{app}$ appears to be smaller than

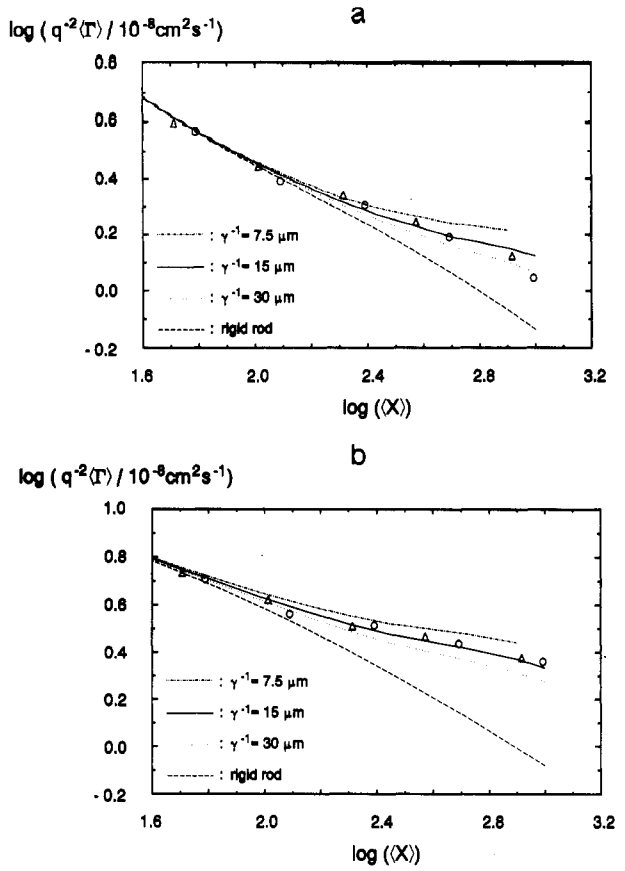


**Figure 3.** Dependence of the apparent diffusion coefficient $D_{app} = \Gamma_{init}/q^2$ on the average degree of polymerization, $\langle X \rangle$, at (a) $\theta = 20°$ and (b) $\theta = 90°$. The experimental data for two different actin concentrations (prep A = 2.5 μM; prep B = 5 μM) are compared with simulated data for rigid and semiflexible rods in dilute solution.

expected from the model calculations. As will be discussed later on in detail, this difference can be put down to a concentration effect.

Besides the polydispersity of the sample, we have to consider another problem when dealing with biological material. We cannot expect that after purification all protein molecules, actin as well as gelsolin, have maintained their biological activity. That means, solutions of the same theoretical molar ratio for actin/gelsolin (as calculated from the protein concentration) may not give the same average filament length, when using different protein preparations. Furthermore, because of the critical actin concentration, the average degree of polymerization depends on the actin concentration. Taking all these considerations into account, we have corrected our theoretical average filament length ([A]:[G]), as obtained from the protein concentrations, according to

$$\langle X \rangle_{cal} = f_X([A]:[G]) \qquad (10)$$

$f_X$ was determined by minimizing the standard deviation of the experimental data with respect to the model calculations, assuming different Kuhn lengths. Considering only solutions with [A]:[G] ≤ 800, where we can probably neglect concentration effects on the correlation function (see below for a detailed discussion), comparison of the initial slope apparent diffusion coefficients results in a Kuhn length of 15 μm. In all figures and throughout the text, we will use [A]:[G] for the theoretical average filament length, as calculated from the protein concentration. But the reader should keep in mind that the actual average degree of polymerization, $\langle X \rangle$, can be calculated using the correction factors, $f_X^A = 1.23$ and $f_X^B = 1.03$, for the two protein preparations.

The apparent diffusion coefficient in eqs 1 and 2 is defined for the slope of the correlation function in the limit of $t \to 0$. The initial decay rate, calculated from the experimental DLS spectra, however is obtained with a finite sampling time. Therefore, we cannot exclude that contributions from higher internal bending modes were not well retrieved by the fitting results of the experimental data. In order to circumvent this problem, we already used the initial decay rate as obtained from a cumulant fit to the calculated correlation function for comparison with the experimental results. Moreover, having calculated the theoretical spectra, we can compare the entire decay profile of the experimental and theoretical correlation functions. In Figure 4, we give such a comparison of experimental spectra with model calculations for different molar ratios of actin/gelsolin at three different scattering angles. For short filament lengths ([A]:[G] = 50) the calculated correlation functions for rigid and semiflexible rods with a persistence length $P \geq 7.5$ μm are almost identical over the entire $q$ range investigated, and the experimental data are well recovered by the model calculations. For longer rods, actin/gelsolin 100:1, the effect of flexibility results in a significantly faster decay of the theoretical correlation function in comparison to the rigid rod model calculations. As expected from eq 2, the difference is more pronounced at higher scattering angles. For $\theta \geq 60°$, the difference in the decay profile exceeds the experimental error for the measured DLS spectra. In this high $q$ range (see Figure 4c), it becomes evident that the experimental data deviate significantly from the rigid-rod model, revealing some flexibility of the rodlike molecules. Going to even longer average filament lengths, the difference in the theoretical DLS spectra for different persistence lengths becomes well resolved. For all scattering angles considered, the correlation functions for semiflexible rods decay much faster than the rigid rod spectra. The influence of internal bending modes increases with increasing scattering vector. Figure 4 indicates that the experimental data for actin/gelsolin 400:1 are well described by the diffusion of semiflexible rods with a persistence length of 7.5 μm, assuming an exponential distribution of the filament lengths. For the lower actin concentration (2.5 μM) the results from [A]:[G] = 800 are also in agreement with the model calculations (data not shown). At higher concentration and for longer filaments however, we observed deviations of the experimental data from model predictions that can be attributed to concentration effects in the semidilute regime.

**Concentration Effects on the Dynamics of Actin Filaments. Dilute Solution; Effect of the Critical Concentration.** In contrast to most synthetic macromolecule the polymerization of F-actin is a reversible dynamic process. Electron microscopy on F-actin indicates that the subunits (actin monomers) have a certain orientation in the helical filaments.[55] The structural polarity and the steady ATP hydrolysis have the consequence that filaments can lengthen on one end and shorten simultaneously on the other end. This reaction is called treadmilling.[56,57] The equilibrium condition is characterized by a constant concentration of G-actin monomers, the critical concentration. Therefore, the average degree of polymerization for a constant ratio of actin/gelsolin is

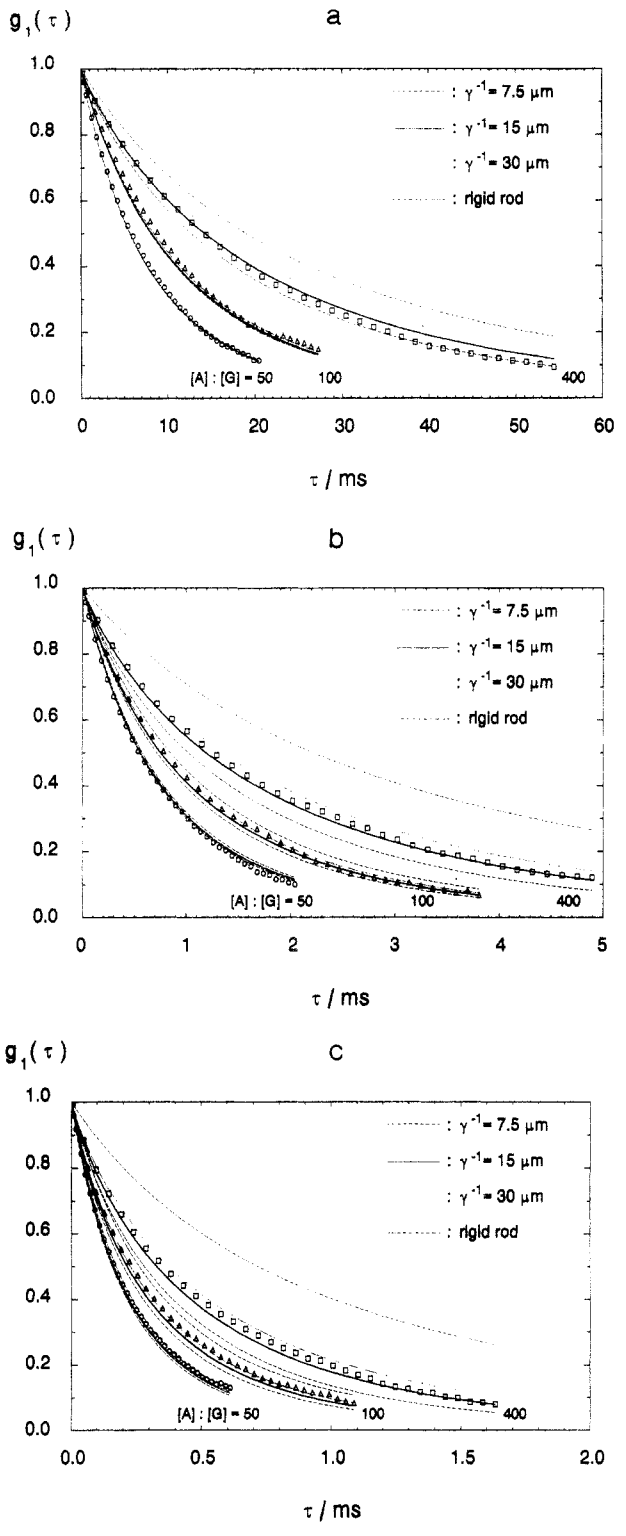


**Figure 4.** Comparison of experimental first-order correlation functions at different scattering angles (a, 20°; b, 60°; and c, 120°) and for different average degrees of polymerization with model calculations for rigid and semiflexible rodlike molecules. Experimental data are shown for prep A ([A] = 5 μM, $f_X^A$ = 1.23).

dependent on the total actin concentration

$$\langle X \rangle \propto \frac{[A]}{[G]}\left(1 - \frac{[A_c]}{[A]}\right) \tag{11}$$

where $[A_c]$ is the critical concentration for the pointed end. The barbed end is blocked by gelsolin. To investigate the influence of $[A_c]$ on the average degree of polymerization, we calculated correlation functions for semiflexible rodlike molecules with the dimensions of actin filaments with different $\langle X \rangle$ and a persistence length of 7.5 μm. For

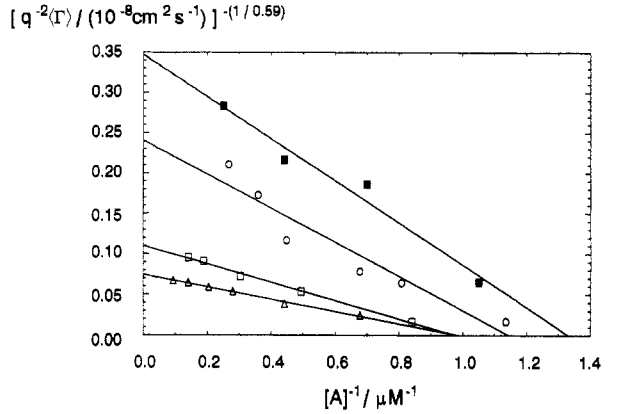


**Figure 5.** Concentration dependence of $\Gamma_{init}/q^2$ for actin filaments with an average degree of polymerization of 50 (△, □) and 150 (○, ■), respectively. Experimental data were obtained from four different actin preparations to determine the critical actin concentration. Measurements were performed at $\theta$ = 20°.

**Table 2. Critical Actin Concentration $[A_c]$ As Obtained from Concentration-Dependent Measurements for Two Different Average Filament Lengths**

| sample | C | D | E | F |
|---|---|---|---|---|
| [A]:[G] | 50 | 50 | 150 | 150 |
| $[A_c]/\mu M$ | 1.0 | 1.0 | 0.87 | 0.75 |

$15 \leq \langle X \rangle \leq 150$ we obtained the following scaling law for the apparent diffusion coefficient

$$D_{app} = \langle \Gamma \rangle q^{-2} \propto \langle X \rangle^{-a} \tag{12}$$

The exponent was estimated to $a$ = 0.59. Equations 11 and 12 give

$$q^{-2}\langle \Gamma \rangle \propto \left[\frac{[A]}{[G]}\left(1 - \frac{[A_c]}{[A]}\right)\right]^{-a} \tag{13}$$

In fact, within the dilute solution regime we observed a strong dependence of the DLS spectra on the total actin concentration. According to eq 13, a plot of $\langle \Gamma \rangle/q^2$ versus 1/[A] will provide the critical actin concentration. Corresponding data are shown in Figure 5 for four different actin and gelsolin preparations. We studied molar ratios of actin/gelsolin of 50:1 and 150:1, respectively. The spectra were measured at a scattering angle of 20°, where $qL \leq 1$, in order to minimize contributions from rotational motion and interference effects from longer filaments. The critical concentration as obtained from the interception with the abscissa is listed in Table 2. The average value of $[A_c]$ = 0.9 μM is in good agreement with reported data from electron microscopy.[58,59]

**Dilute and Semidilute Regime with Consideration of the Critical Concentration.** To study the thermodynamic and hydrodynamic effects on the mutual diffusion coefficient at different filament concentrations, we prepared solutions of actin/gelsolin with a constant degree of polymerization according to

$$[A_F]:[G] = 300 \tag{14}$$

with

$$[A_F] = [A] - [A_c] \tag{15}$$

where $[A_F]$ is the concentration of filamentous actin. For the critical actin concentration we assumed $[A_c]$ = 0.9 μM (see Table 2). We studied F-actin solutions within a concentration range from 2.2 to 105 μM which corresponds to $3.8 \leq c\langle L \rangle^3 \leq 169$. Correlation functions were measured at two different scattering angles, $\theta$ = 20° and $\theta$ = 90°, respectively. Within the experimental error, for $c\langle L \rangle^3 \leq$ 10 the apparent diffusion coefficient is independent on

concentration. From the corresponding DLS spectra at $\theta = 90°$ (data not shown) it became obvious that not only the initial decay rate but the entire decay profile of the correlation functions is identical for all three solutions.

In dilute solution, the mutual diffusion coefficient is concentration dependent due to thermodynamic and hydrodynamic effects[60]

$$D = D_0(1 + k_D c) \tag{16}$$

with

$$k_D = 2A_2M - k_f - \nu \tag{17}$$

Here, $k_D$ is the diffusion virial coefficient, $A_2$ the second osmotic virial coefficient, $k_f$ accounts for increased friction due to hydrodynamic interactions, and $\nu$ is the partial specific volume of the solute. In general, steric rod–rod interactions lead to a decrease in the translational diffusion coefficient and hence to a positive value for $k_f$. The thermodynamic interaction parameter $A_2$ might be either positive (repulsive potential) or negative (attractive) in sign. Accordingly, the mutual translational diffusion coefficient can either increase or decrease with concentration. $k_D = 0$ means that both, the hydrodynamic and thermodynamic effect, cancel. For actin/gelsolin solutions with $c\langle L\rangle^3 \leq 10$ we obtained a negligible slope, which has been previously observed for other proteins in the dilute solution regime.[61,62]

Therefore, we assume that, for the actin/gelsolin system studied here, the dilute solution regime covers at least the range up to $c\langle L\rangle^3 = 10$. This finding is in agreement with data reported on PBLG by Tracy and Pecora,[63] who found the transition to semidilute solution in DMF taking place at $cL^3 = 17$. Similar values were obtained for PBLG in dichloroethane[64] and in aqueous DNA solutions.[65,66] The experimental results have been confirmed by Brownian dynamics simulations on rodlike polymers.[67,68] For the actin/gelsolin system one has to remember that we are dealing with a rather broad distribution of filament lengths. That means, in solution we have a number of longer actin filaments but also shorter molecules compared to $\langle L\rangle$. There is no theory available considering the effect of polydispersity on the dilute–semidilute transition but our results suggest that using the number-averaged lengths for calculating $c\langle L\rangle^3$ gives a consistent picture for the transition range in comparison to rather monodisperse polymer system.

Going to higher concentration ($[A_F] \geq 22$ μM), we observed an almost constant apparent diffusion coefficient as obtained from the DLS data at $\theta = 20°$. At higher scattering vector ($\theta = 90°$) however, $\langle\Gamma\rangle/q^2$ decreased significantly with concentration, and hence, as shown in Figure 6, for $20 < c\langle L\rangle^3 < 170$ the ratio $D_{app}(\theta=90°)/D_{app}(\theta=20°)$ decreases with concentration. Assuming that eq 16 is applicable also to the semidilute regime, and that it provides for both, the translational and rotational diffusion coefficient, the same diffusion virial coefficient, we would expect a constant value for the ratio $D_{app}(\theta=90°)/D_{app}(\theta=20°)$. Our results suggest that rotational and translational motion experience a different concentration dependence. For $\theta = 20°$ the value of $q\langle L\rangle$ is calculated to 5.9 (see Table 1) for $\langle X\rangle = 350$, indicating that at low scattering angle the rotational motion from most of the filaments probably gives only a minor contribution to the correlation function. At $\theta = 90°$ however, $q\langle L\rangle$ increases to 23.8, and now the higher terms in eq 2 give stronger contributions to the scattered intensity. Neglecting the concentration effect on the internal bending motion, the decrease in $D_{app}(\theta=90°)/D_{app}(\theta=20°)$ suggests that the rotational motion experienced a stronger restriction than

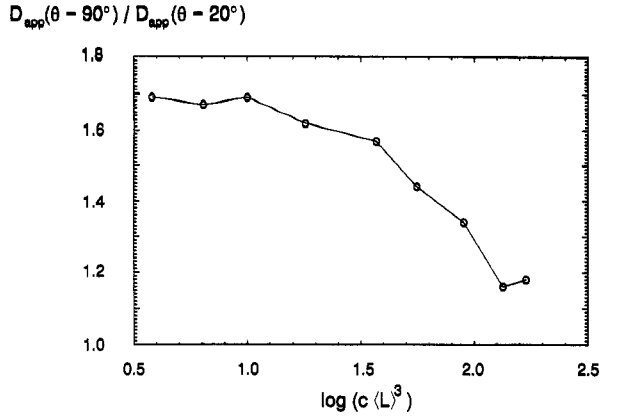


**Figure 6.** Ratio of the apparent diffusion coefficients $D_{app}(\theta=90°)/D_{app}(\theta=20°)$ versus $\log[c\langle L\rangle^3]$ in dilute and semidilute solution. The average filament length was chosen $[A_F]:[G] = 300$.

the translational diffusion process. The decrease of the apparent diffusion coefficient at $\theta = 90°$ indicates that $k_\theta < k_D$, where $k_D$ is probably close to zero. (See dilute solution regime and results at low scattering angle.)

Very similar results were obtained by Fujime et al. for semidilute solutions of the fd virus.[69] The virus is a semiflexible macromolecule with a length of about 890 nm and a diameter of 9 nm. Comparison with Table 1 reveals that these dimensions are very similar to the average length and diameter of our actin/gelsolin system with a molar ratio of 300:1. Fujime et al. performed DLS measurements up to $cL^3 = 160$ and found that at low scattering angle the apparent diffusion coefficient slightly increased with concentration while for $\theta > 30°$ it decreased. Their findings are in qualitative agreement with our results shown in Figure 6. Fujime et al. concluded that probably the lengthwise and sidewise translational motions are not much restricted with concentration, whereas the rotation of the molecules is slowed down at high $cL^3$. By introducing a scaling parameter $\beta$ in eq 2 to reduce the rotational diffusion coefficient they obtained a good agreement between the decay profile of experimental and calculated correlation functions. Fairly recent transient electric birefringence measurements of the fd virus support their conclusions. Kramer et al.[70] found that at high ionic strength, where the Coulomb interaction between the molecules is screened, the rotational diffusion coefficient decreases with concentration. Within the intermediate concentration range their results are in agreement with the relationship

$$\theta/\theta_0 = [1 + \beta^{-1/2}(cL^3)]^{-2} \tag{18}$$

proposed by Teraoka and Hayakawa,[71,72] where $c$ is the number concentration of the solute molecules.

A different approach to the semidilute solution problem was given by Maeda.[20] He assumed that the second virial coefficient $A_2$ is a function of $qL$. Accordingly, each diffusion coefficient in eqs 1 and 2 can be expressed by $D_\parallel A(qL,c)$, $D_\perp A(qL,c)$, and $\theta A(qL,c)$, respectively. $A(qL,c)$ is common for all transport coefficients, but the hydrodynamic effect on each motion might be different. Equation 16 will change to

$$D = D_0(1 + k_D(qL)c) \tag{19}$$

with

$$k_D(qL) = 2A_2(qL)M - k_f(qL) - \nu \tag{20}$$

where the parameter $k_D$ is now a function of $qL$. Obviously, by introducing a length-dependent osmotic virial coefficient, Maeda accounts for the fact that at low scattering

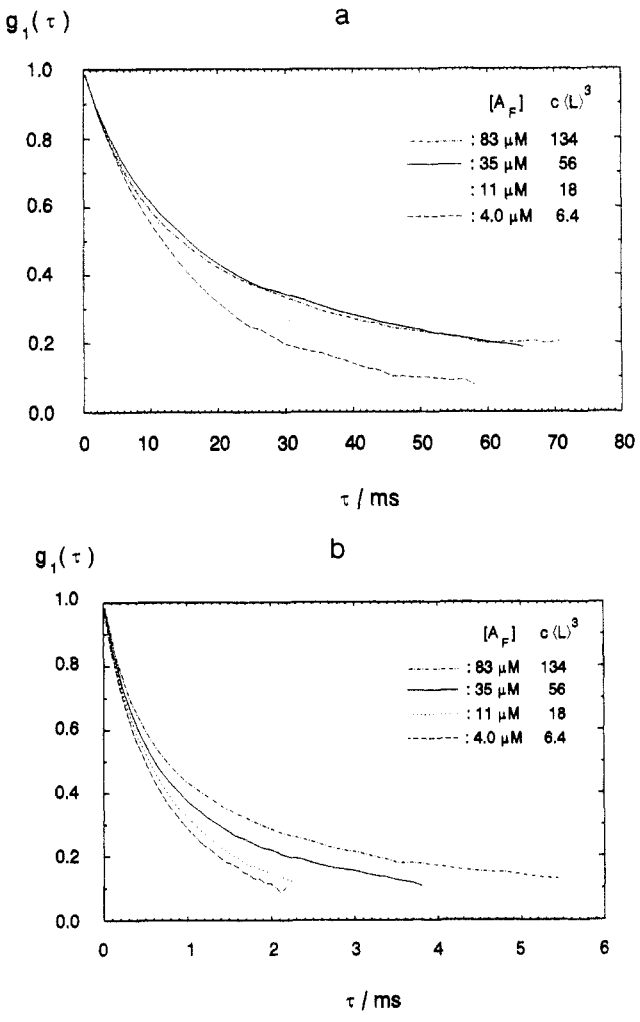


**Figure 7.** First-order correlation function profile in semidilute solution for $[A_F]$:[G] = 350 at two different scattering angles; (a) $\theta = 20°$ and (b) $\theta = 90°$.

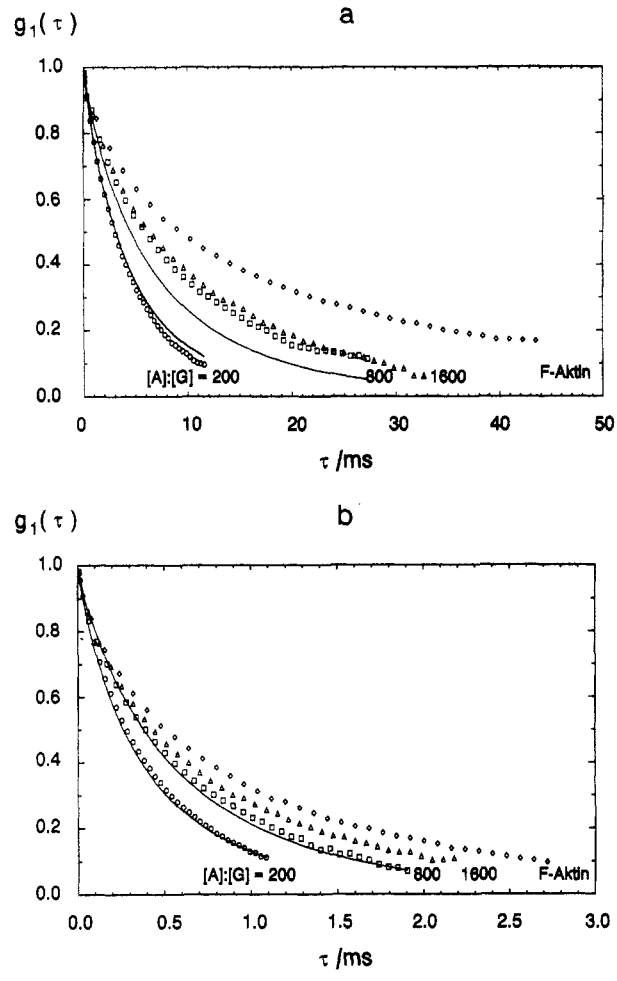


**Figure 8.** First-order correlation functions for actin filaments capped with gelsolin in comparison with pure F-actin: (a) $\theta = 35°$ and (b) $\theta = 120°$. The solid lines correspond to model calculations for semiflexible rods with $\gamma^{-1} = 15$ μm. The actin concentration was $[A_F] \leq 2.5$ μM.

vector the scattered intensity results from fluctuations of the system while at high $q$ microscopic relaxation processes give stronger contributions. Our experimental results, shown in Figure 6, are in qualitative agreement with Maeda's prediction that the diffusion virial coefficient is a decreasing function of $qL$. At low scattering angles the repulsive thermodynamic interaction between the rods can compensate the slowdown of the diffusional motion by frictional effects (positive $k_f$). Assuming a stronger dependence of $k_D$ than $k_f$ on the scattering vector results in a decrease of $D_{app}$ with increasing $qL$. In other words, the hydrodynamic effect becomes dominant over the influence of the second virial coefficient on the dynamics of the rodlike molecules. Similar experimental results were obtained by DLS studies on PBLG in DMF[73] and on the fd virus[68] in aqueous solution. Although, a physical basis for eqs 19 and 20 is still lacking.

In addition to changes in the initial slope, we observed a slow component arising in the time correlation function of concentrated solution of actin/gelsolin in the semidilute regime. Figure 7 shows experimental data at different actin concentrations for $\theta = 20°$ and $\theta = 90°$, respectively. The average degree of polymerization $\langle X \rangle = 350$ was obtained from comparison of the experimental $D_{app}$ in the dilute solution regime ($[A_F] \leq 6.5$ μM) with calculated values for semiflexible rods. As Figure 7 indicates, the contribution of the slow relaxation process increased with actin concentration. A comparison of Figure 7, parts a and b, shows a more pronounced concentration dependence at $\theta = 20°$. Detailed angular dependent measurements (data not shown) confirmed that the amplitude of the slow mode diminished with increasing scattering angle. The nature of the slow relaxation mode, seen in a number of polymer systems, is still under debate. It is either attributed to cooperative motion (e.g. cluster formation) or an interdiffusional process.[74,75] Although, we did not test for $q^2$ dependence, the angular dependence of the slow mode indicates that the fluctuations occur over a length scale large compared to the inverse scattering vector (~200 nm at low scattering angles).

For the two highest concentrations ($[A_F] > 80$ μM) studied, our experimental results indicate that the apparent diffusion coefficient slightly increased at low scattering vector, while at $\theta = 90°$, $D_{app}$ seems to level off. A possible explanation is that the sidewise translational diffusion of the rodlike molecules becomes severely restricted. As a consequence, the rodlike molecules can move perpendicular to their rod axis only in a cooperative manner, giving rise to the slow mode in the polarized DLS spectra. At the same time, the diffusion coefficient for lengthwise translational motion might increase due to repulsive rod–rod interactions, resulting in a slight increase of $D_{app}$ at low scattering angle. The decrease in $D_\perp$ has been observed in a Brownian dynamics simulation of rodlike polymers, but an increase of $D_\parallel$ was not observed.[67] It is possible that in our case, because we are dealing with charged molecules, electrostatic effects become important in the concentrated regime and give rise to additional repulsive forces between the rods. More detailed concentration-dependent measurements in the semidilute–

concentrated solution regime are currently under investigation.

**Transition to Unmodified F-Actin.** For a complete description of the dynamics of the F-actin in solution, we have measured very long filaments with a molar ratio of [A]:[G] = 1600 and pure F-actin. The large value for $c\langle L\rangle^3 = 53$ ($[A_F] = 2.5\ \mu M$) and the length of the filaments ($\gamma\langle L\rangle = 0.30$) means that a quantitative description within the model for semiflexible rods is not feasible. However, a comparison of the experimental time correlation functions at $\theta = 35°$ and $\theta = 120°$, shown in Figure 8, with the results on shorter filaments gives valuable information about the structure and dynamics of F-actin. At both scattering angles the correlation function of pure F-actin decays much slower than for [A]:[G] = 1600. Therefore, we can conclude that the average filament length for unmodified F-actin, as obtained under our experimental conditions, exceeds significantly 5.5 $\mu$m; we calculated for $\langle X\rangle = 1970$ (considering $f_X^A = 1.23$). Otherwise, the dynamics of F-actin are qualitatively very similar to those of the shorter filaments. The appearance of the slow mode in the correlation function became clearly discernible at $\theta = 35°$, and the contribution decreased significantly with increasing scattering angle. Our experimental results on F-actin of different average filament lengths suggest that the microfilaments are rather stiff, and therefore, we give a strong preference for modeling the cytoskeleton as a network composed of rigid rodlike macromolecule.

**Acknowledgment.** We are grateful to Dr. Tadekazu Maeda for the computer programs to calculate the dynamic structure factor of rigid and semiflexible rodlike molecules. We are indebted to the Deutsche Forschungsgemeinschaft (SFB 223) for financial support.

## References and Notes

(1) Korn, E. D. *Physiol. Rev.* **1982**, *62*, 672.
(2) Pollard, D. T.; Cooper, J. A. *Ann. Rev. Biochem.* **1986**, *55*, 987.
(3) DeRosier, D. J.; Tilney, L. G. *The Form and Function of Actin: in Cell and Muscle Motility V, The Cytoskeleton*; Plenum Press: New York, 1984.
(4) Stossel, T. P.; Chaponnier, C.; Ezzel, R. M.; Hartwig, J. H.; Janmey, P. A.; Kwiatkowski, D. J.; Lind, S. E.; Smith, D. B.; Southwick, F. S.; Yin, H. L.; Zaner, K. S. *Ann. Rev. Cell Biol.* **1985**, *1*, 353.
(5) Jen, C. J.; McIntire, L. V.; Bryan, J. *Arch. Biochem. Biophys.* **1982**, *216*, 126.
(6) Sato, M.; Leimbach, G.; Schwarz, W. H.; Pollard, T. D. *J. Biol. Chem.* **1985**, *260*, 8585.
(7) Zaner, K. S.; Stossel, T. P. *J. Cell. Biol.* **1982**, *93*, 987.
(8) Doi, M.; Edwards, S. F. *The Theory of Polymer Dynamics*; Clarendon Press: Oxford 1986.
(9) Luby-Phelps, K.; Lanny, F.; Taylor, D. L. *Ann. Rev. Biophys. Chem.* **1988**, *17*, 3699.
(10) Carlson, F. D.; Fraser, A. B. *J. Mol. Biol.* **1974**, *89*, 273.
(11) Newman, J.; Carlson, F. D. *Biophys. J.* **1980**, *29*, 37.
(12) Fujime, S.; Takasaki-Oshita, M.; Ishiwata, S. *Biophys. Chem.* **1987**, *27*, 211.
(13) Seils, J.; Jockusch, B. M.; Dorfmüller, Th. *Biopolymers* **1990**, *30*, 677.
(14) Schmidt, C. F.; Bärmann, M.; Isenberg, G.; Sackmann, E. *Macromolecules* **1989**, *22*, 3638.
(15) Hinssen, H. *Fortschr. Zool.* **1987**, *34*, 52.
(16) Janmey, P. A.; Chaponnier, C.; Lind, S. E.; Zaner, K. S.; Stossel, T. P.; Yin, H. L. *Biochemistry* **1985**, *24*, 3714.
(17) Coué, M.; Korn, E. D. *J. Biol. Chem.* **1985**, *260*, 15033.
(18) Yin, H.; Zaner, K. S.; Stossel, T. P. *J. Biol. Chem.* **1980**, *255*, 9494.
(19) Janmey, P. A.; Peetermans, J.; Zaner, K. S.; Stossel, T. P.; Tanaka, T. *J. Biol. Chem.* **1986**, *261*, 8357.
(20) Maeda, T. *Macromolecules* **1989**, *22*, 1881.
(21) Fujime, S.; Maeda, T. *Macromolecules* **1985**, *18*, 191.
(22) Maeda, T.; Fujime, S. *Macromolecules* **1985**, *18*, 2430.
(23) Yanagida, T.; Nakase, M.; Nishiyama, K.; Oosawa, F. *Nature* **1983**, *307*, 58.
(24) Takebayashi, T.; Morita, Y.; Oosawa, F. *Biochem. Biophys. Acta* **1977**, *492*, 357.
(25) Drögemeier, J.; Eimer, W. *Macromolecules*, following paper in this issue.
(26) Pecora, R. *J. Chem. Phys.* **1964**, *40*, 1604.
(27) Tracy, M.; Pecora, R. *Ann. Rev. Phys. Chem.* **1992**, *43*, 525.
(28) Schaefer, D. W.; Bendek, G. B.; Schofield, P.; Bradford, E. *J. Chem. Phys.* **1971**, *35*, 3884.
(29) Wilcoxon, J.; Schurr, J. M. *Biopolymers* **1983**, *22*, 849.
(30) Aragon, S.; Pecora, R. *J. Chem. Phys.* **1985**, *82*, 5346.
(31) Doi, M.; Shimada, T.; Okano, K. *J. Chem. Phys.* **1988**, *88*, 4070.
(32) Maeda, T.; Fujime, S. *Macromolecules* **1984**, *17*, 1157.
(33) Maeda, T.; Fujime, S. *Macromolecules* **1984**, *17*, 2381.
(34) Kubota, K.; Tominaga, Y.; Fujime, S. *Biopolymers* **1987**, *26*, 1717.
(35) Tirado, M. M.; García de la Torre, J. *J. Chem. Phys.* **1979**, *71*, 2581.
(36) Tirado, M. M.; García de la Torre, J. *J. Chem. Phys.* **1980**, *73*, 1986.
(37) Tirado, M. M.; Martínez, C. L.; García de la Torre, J. *J. Chem. Phys.* **1984**, *81*, 2047.
(38) Yamakawa, H.; Fujii, M. *Macromolecules* **1973**, *6*, 407.
(39) Schmidt, M.; Stockmayer, W. H. *Macromolecules* **1984**, *17*, 509.
(40) Hagerman, P. J.; Zimm, B. H. *Biopolymers* **1981**, *20*, 1481.
(41) Song, L.; Kim, U.-G.; Wilcoxon, J.; Schurr, J. M. *Biopolymers* **1991**, *31*, 547.
(42) Aragon, S. *Macromolecules* **1991**, *24*, 3453.
(43) Spudich, J. A.; Watt, S. *J. Biol. Chem.* **1971**, *246*, 4866.
(44) Hinssen, H.; Small, J. V.; Sobieszek, A. *FEBS Lett.* **1984**, *166*, 90.
(45) Pope, B.; Gooch, J.; Hinssen, H.; Weeds, A. G. *FEBS Lett.* **1989**, *259*, 185.
(46) Koppel, D. E. *J. Chem. Phys.* **1972**, *57*, 4841.
(47) Provencher, S. W. *J. Chem. Phys.* **1976**, *64*, 2772.
(48) Provencher, S. W. *Comput. Phys. Commun.* **1982**, *27*, 213.
(49) Provencher, S. W. *Comput. Phys. Commun.* **1982**, *27*, 229.
(50) Egelman, E. H. *J. Muscle Res. Cell Motil.* **1985**, *6*, 129.
(51) Holmes, H. C.; Popp, D.; Gebhard, W.; Kabsch, W. *Nature* **1990**, *347*, 44.
(52) Egelman, E. H.; Padron, R. *Nature* **1984**, *307*, 56.
(53) Drögemeier, J. Ph.D. Thesis, University of Bielefeld, 1992.
(54) Elias, H.-G. *Makromoleküle*, Bd. 1; Hüthig & Wepf Verlag: Basel, Heidelberg, New York, 1990.
(55) Moore, P. B.; Huxley, H. E.; DeRosier, D. J. *J. Mol. Biol.* **1970**, *50*, 279.
(56) Pantaloni, D.; Hill, T. L.; Carlier, M.-F.; Korn, E. D. *Proc. Natl. Acad. Sci. U.S.A.* **1985**, *82*, 7207.
(57) Korn, E. D. *Fortschr. Zool.* **1987**, *34*, 65.
(58) Tsukita, S.; Ishikawa, H. *J. Cell Biol.* **1984**, *98*, 1102.
(59) Cooper, J. A.; Buhle, E. L., Jr.; Walker, S. B.; Tsong, T. Y.; Pollard, T. D. *Biochemistry* **1983**, *22*, 2193.
(60) Yamakawa, H. *Modern Theory of Polymer Dynamics*; Harper and Row: New York, 1971.
(61) Patkowski, A.; Seils, J.; Hinssen, H.; Dorfmüller, Th. *Biopolymers* **1990**, *30*, 427.
(62) Eimer, W.; Niermann, M.; Eppe, M.; Jockusch, B. M. *J. Mol. Biol.* **1993**, *229*, 146.
(63) Tracy, M. A.; Pecora, R. *Macromolecule* **1992**, *25*, 337.
(64) Zero, K. M.; Pecora, R. *Macromolecule* **1982**, *15*, 87.
(65) Goinga, H. T.; Pecora, R. *Macromolecule* **1991**, *24*, 6128.
(66) Wang, L.; Garner, M. M.; Yu, H. *Macromolecule* **1991**, *24*, 2368.
(67) Bitsanis, I.; Davis, H. T.; Tirrell, M. *Macromolecule* **1988**, *21*, 2824.
(68) Bitsanis, I.; Davis, H. T.; Tirrell, M. *Macromolecule* **1990**, *23*, 1157.
(69) Fujime, S.; Takasaki-Oshita, M.; Maeda, T. *Macromolecule* **1987**, *20*, 1292.
(70) Kramer, H.; Deggelmann, M.; Graf, C.; Hagenbüchle, M.; Johner, C.; Weber, R. *Macromolecule* **1992**, *25*, 4325.
(71) Teraoka, I.; Ookubo, N.; Hayakawa, R. *Phys. Rev. Lett.* **1985**, *55*, 2712.
(72) Teraoka, I.; Hayakawa, R. *J. Chem. Phys.* **1989**, *91*, 2643.
(73) Russo, P. S.; Karasz, F. E.; Langley, K. H. *J. Chem. Phys.* **1984**, *80*, 5312.
(74) Ferrari, M. E.; Bloomfield, V. A. *Macromolecule* **1992**, *25*, 5266.
(75) Richtering, W.; Gleim, W.; Burchard, W. *Macromolecule* **1992**, *25*, 3795.